New Journal of Physics
The open access journal at the forefront of physics
Deutsche Physikalische Gesellschaft DPG | IOP Institute of Physics

Orbital correlations and dimensional crossover in epitaxial $Pr_{0.5}Ca_{0.5}MnO_3/La_{0.5}Sr_{0.5}MnO_3$ superlattices

H Wadati[1], J Okamoto[2], M Garganourakis[3], V Scagnoli[3], U Staub[3], E Sakai[2], H Kumigashira[2], T Sugiyama[4], E Ikenaga[4], M Nakamura[5], M Kawasaki[1,5] and Y Tokura[1,5]

[1] Department of Applied Physics and Quantum-Phase Electronics Center (QPEC), University of Tokyo, Hongo, Tokyo 113-8656, Japan
[2] Condensed Matter Research Center and Photon Factory, Institute of Materials Structure Science, High Energy Accelerator Research Organization, Tsukuba 305-0801, Japan
[3] Swiss Light Source, Paul Scherrer Institut, 5232 Villigen PSI, Switzerland
[4] Japan Synchrotron Radiation Research Institute, SPring-8, Hyogo 679-5198, Japan
[5] RIKEN Center for Emergent Matter Science (CEMS), Wako 351-0198, Japan
E-mail: wadati@ap.t.u-tokyo.ac.jp

Received 17 March 2014, revised 18 June 2014
Accepted for publication 23 June 2014
Published 30 July 2014

New Journal of Physics **16** (2014) 073044

doi:10.1088/1367-2630/16/7/073044

Abstract

We studied the charge-orbital ordering in the superlattice of charge-ordered insulating $Pr_{0.5}Ca_{0.5}MnO_3$ and ferromagnetic metallic $La_{0.5}Sr_{0.5}MnO_3$ by resonant soft x-ray diffraction (RSXD) and hard x-ray photoemission spectroscopy (HXPES). A temperature-dependent incommensurability is found in the orbital ordering by RSXD. In addition, a large hysteresis is observed that is caused by phase competition between the insulating charge ordered and metallic ferromagnetic states. No magnetic phase transitions are observed in contrast to pure $Pr_{0.5}Ca_{0.5}MnO_3$ thin films, confirming the unique character of the superlattice. Mn 2*p* HXPES spectra revealed a hysteresis in the metalicity, supporting the picture of phase competition. The deviation from the commensurate orbital order can be directly related to the decrease of ordered-layer thickness that leads to dimensional crossover from three-dimensional to two-dimensional orbital ordering.

Keywords: resonant soft x-ray diffraction, hard x-ray photoemission spectroscopy, $Pr_{0.5}Ca_{0.5}MnO_3$, $La_{0.5}Sr_{0.5}MnO_3$, superlattices

1. Introduction

Hole-doped perovskite manganites $RE_{1-x}A_xMnO_3$, where RE is a rare-earth (RE = La, Nd, Pr) and A is an alkaline-earth atom (A = Sr, Ba, Ca), have attracted much attention because they exhibit remarkable physical properties such as colossal magnetoresistance (CMR) and complex electronic ordering phenomena [1–8]. $La_{1-x}Sr_xMnO_3$ has a large bandwidth, and a ferromagnetic metallic (FM) ground state is realized for approximately $0.2 \lesssim x \lesssim 0.5$ [9]. The ferromagnetic transition temperatures (T_C) are ~370 K at $x = 0.4$ and 0.5 [8, 9]. Most of the half-doped manganites ($x \simeq 0.5$) with a small bandwidth exhibit the so-called 'CE-type' charge and orbitally ordered (CO/OO) insulating and antiferromagnetic (AF) ordering with alternating Mn^{3+} and Mn^{4+} states within the (001) plane in the form of stripes [10]. This ordering competes with the FM phase. Phase competition between ordered phases is an interesting phenomenon and leads to intriguing behaviors such as CMR and nanometer-scale phase separation. These ordering phenomena lead to symmetry lowering and a doubling of the unit cell, which results in superlattice reflections observable with different scattering techniques. For higher doping levels $x > 0.5$, the doping leads to orderings that are incommensurate with the ordering wave vector proportional to the doping concentration [11, 12].

In recent years, epitaxially grown films of manganites have been extensively studied. It was found that $La_{1-x}Sr_xMnO_3$ thin films are ferromagnetic for approximately $0.2 \lesssim x \lesssim 0.5$, almost the same as the bulk [13, 14]. Half-doped manganite thin films often remain charged and orbitally ordered, but the physical properties might depend on the strain, that is, the lattice constant and orientation of the substrates. A transition between CO and FM states was observed in $Nd_{0.5}Sr_{0.5}MnO_3$ thin films on $SrTiO_3$ substrates only when the substrate orientation was (011) [15, 16]. Also, in $Pr_{0.5}Ca_{0.5}MnO_3$ thin films, epitaxial strain strongly affects the electronic properties, and the thin films grown epitaxially on $(LaAlO_3)_{0.3}(SrAl_{0.5}Ta_{0.5}O_3)_{0.7}$(LSAT) (011) substrates exhibit a CO transition around 220 K, similar to bulk samples [17].

Interesting phenomena occur when these two systems are brought in direct contact. Results on such stackings have recently been reported by Nakamura *et al* [18]. They fabricated superlattices of $La_{0.5}Sr_{0.5}MnO_3$ (LSMO) and $Pr_{0.5}Ca_{0.5}MnO_3$ (PCMO) on LSAT (011) substrates [18]. Pure LSMO and PCMO thin films on LSAT (011) substrates show FM ($T_C \sim$ 310 K) and CO ($T_{CO} \sim$ 220 K), respectively. They found that they could control the phase boundary at the interface between the FM LSMO and the AF and CO/OO PCMO by applying magnetic fields or changing the individual layer thicknesses. In addition, they observed superlattice reflections indicative of the structural distortions induced by the charge and orbital order in these systems. With the case of thicker LSMO than PCMO layers, FM states dominate, whereas with thicker PCMO than LSMO layers, CO states dominate. Particularly interesting is the case with equal thicknesses. In that case, the reflections exhibit a strong hysteresis behavior even in a zero magnetic field, direct evidence for the first-order phase transition between these competing phases.

To gain more insight into these problems of phase transitions and phase competitions, we investigated the charge-orbital ordering in [PCMO (5 layers)/LSMO (5 layers)]$_{15}$ superlattices by resonant soft x-ray diffraction (RSXD). This technique combines the sensitivity of the Mn $2p \rightarrow 3d$ electronic transition to the electronic and magnetic properties of the transition metal $3d$ states with the sensitivity to the long-range order of diffraction. Historically, resonant x-ray diffraction at the Mn 1 s edge was first employed to study CO/OO states in manganites [19]. This technique was expected to reflect the Mn $3d$ states by the Coulomb interaction between $3d$

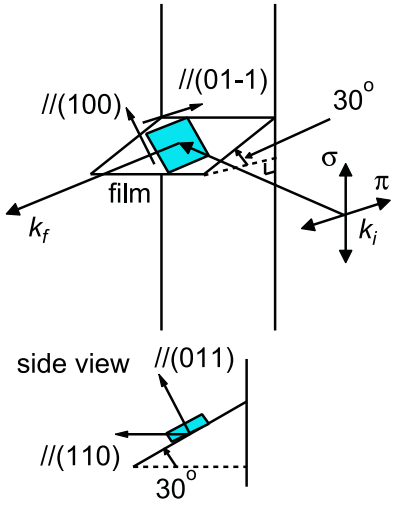

Figure 1. The experimental geometry with the [110] axis of the PCMO/LSMO superlattice in the scattering plane and using a simple cubic perovskite cell notation.

and 4*p* electrons [20], but band-structure calculations revealed that this directly probes lattice distortion because Mn 4*p* states strongly hybridize with neighboring O 2*p* states and are thus influenced by lattice distortion [21, 22]. However, RSXD at the Mn 2*p* edge can directly reflect Mn 3*d* states, and is extremely sensitive to even small details in the electronic orderings. RSXD has been successfully used to disentangle magnetic and orbital ordering phenomena in manganites [23–33], and is especially sensitive to the magnetic structures in thin films when using giant resonant enhancement at the Mn 2*p* edge [31–34]. There has recently been a study of imprinting magnetic and electronic information in epitaxially grown PCMO films [32].

In the present study, we find a significant hysteresis behavior of the superlattice reflection that is sensitive to the orbital order of the Mn 3*d* states. In addition, the system shows a clear temperature dependence of the ordering wave vector on hysteresis behaviors. Such hysteresis was also observed in the metalicity from Mn 2*p* photoemission spectra. The temperature-dependent incommensurability in the orbital ordering can be related to the change of orbital coupling through the FM metallic layer centered around the LSMO layer, that is, dimensional crossover from three-dimensional (3D) to two-dimensional (2D) ordering with increasing temperature.

2. Experiment

[PCMO (5 layers)/LSMO (5 layers)]$_{15}$ superlattices were grown on the (011) surface of an LSAT substrate by pulsed laser deposition. The details of the sample fabrication were described elsewhere [18]. RSXD experiments were performed on the RESOXS end station [35] at the surface-interface microscopy (SIM) beam line [36] of the Swiss Light Source of the Paul Scherrer Institut, Switzerland. The experimental geometry is shown in figure 1, which is the same as that in [33]. A continuous helium-flow cryostat allows measurements between 25 and 300 K. The experiments were performed in the out-of-focus mode with a beam of approximately 2 × 2 mm^2.

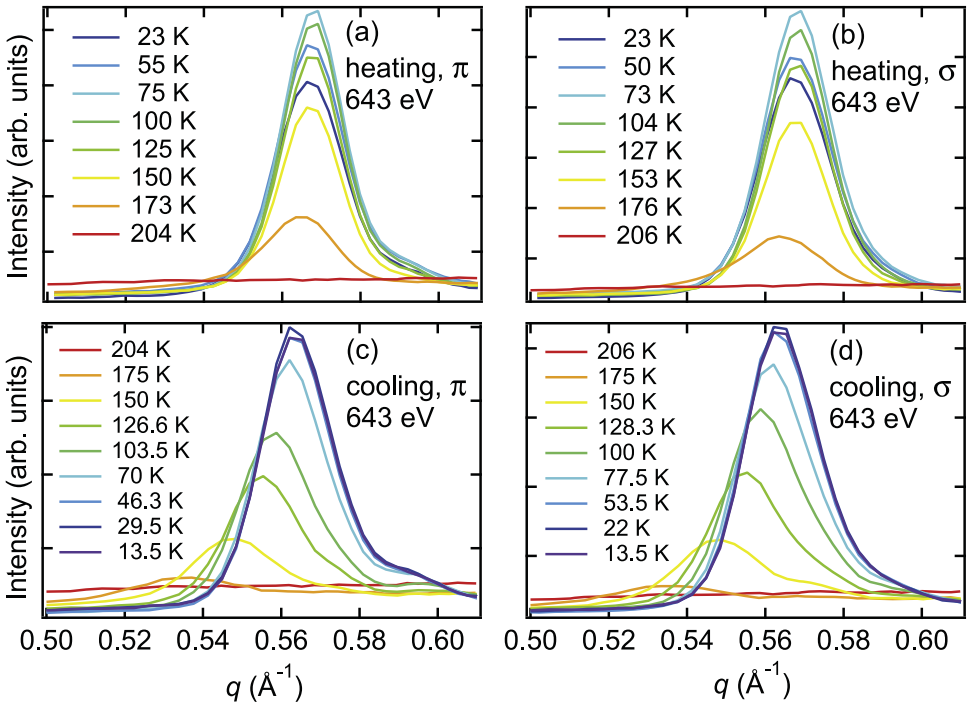

Figure 2. Temperature dependence of the (hh0) peak. Panels (a) and (b) ((c) and (d)) were measured in the heating (cooling) cycle. Incident x-ray polarizations were π in (a) and (c) and σ in (b) and (d). All the data were taken at $h\nu = 643$ eV (Mn $2p_{3/2} \rightarrow 3d$ absorption edge).

We also performed hard x-ray photoemission spectroscopy (HXPES) measurements to obtain information on the metallic states in LSMO layers. HXPES measurements were carried out at BL47XU of SPring-8. The HXPES spectra were recorded using a Scienta R-4000 electron energy analyzer with a total energy resolution of 250 meV at the photon energy of 7.94 keV. The position of the Fermi level (E_F) was determined by measuring the spectra of gold, which was in electrical contact with the sample. Here again, we used a continuous helium-flow cryostat to cool the sample.

3. Results and discussion

Figure 2 shows the q dependence of the orbital order (hh0) reflection in a simple cubic perovskite notation for various temperatures at the Mn $2p_{3/2}$ edge (643 eV) for both π and σ incoming x-ray polarizations. This reflection has been studied in detail in $Pr_{1-x}Ca_xMnO_3$ bulk manganites and epitaxial grown films [26, 28, 30, 32, 33], and has been shown to be sensitive to both the orbital and magnetic orderings of the systems. The temperature dependence of this reflection in a heating run (panels (a) and (b)) significantly deviates from that in a cooling run (panels (c) and (d)). The reflection appears below ~200 K, which is almost the same as the pure PCMO thin film [33]. There is almost no difference between π (a, c) and σ (b, d) polarizations. The temperature variation of the corresponding peak intensity, the correlation length, and positions are summarized in figure 3. The correlation length ξ is obtained from the full width at half-maximum (FWHM) Δq through $\xi = 2\pi/\Delta q$. In all of these quantities, a large hysteresis is

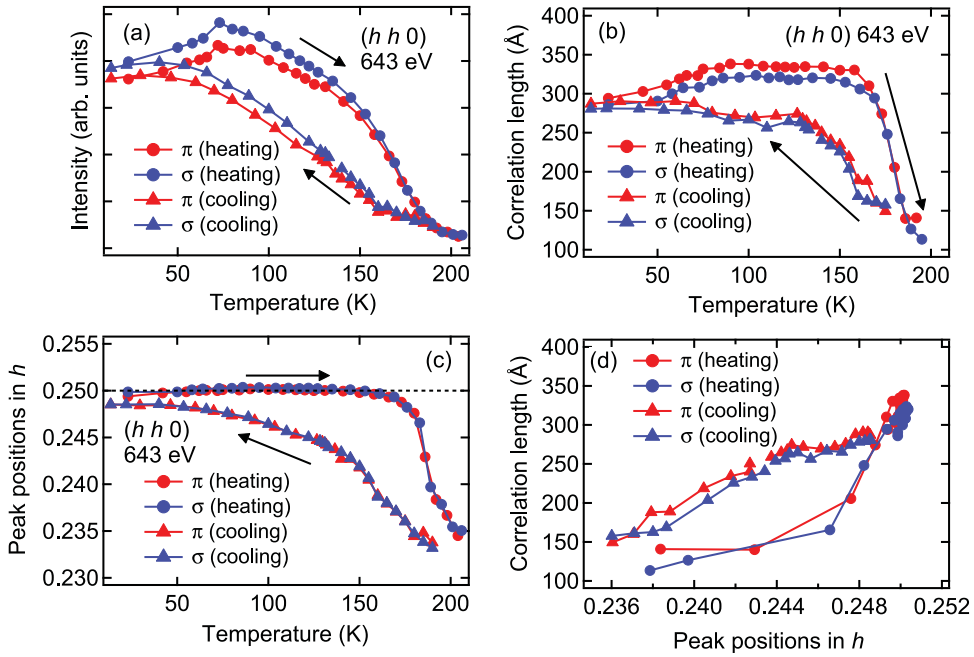

Figure 3. Temperature dependence of the (*hh*0) peak intensity (a), correlation length (b), and positions (c). In panel (d), the correlation length is plotted as a function of peak positions.

observed between cooling and heating cycles. The peak intensity monotonically increases for decreasing temperatures in contrast to the heating cycle, where, interestingly, it first increases and then decreases before it disappears around 200 K. Most interesting is that this is related to both the temperature dependence of the position and FWHM of the reflection. The peak position is incommensurate and temperature dependent in the full range of the cooling cycle. In contrast, the position remains frozen until temperatures of approximately 170 K for the heating cycle. Since the peak position of this reflection type has been found to be related to the doping level [29], it might reflect an *effective* doping in the PCMO layer, which is slightly larger than 0.5 and is temperature dependent. Such interfacial effects were also observed by neutron reflectometry on $La_{2/3}Sr_{1/3}MnO_3/Pr_{2/3}Ca_{1/3}MnO_3$ multilayers [37], where a ferromagnetic moment was found to occur in the $Pr_{2/3}Ca_{1/3}MnO_3$ layers, although the concentrations of the component layers were different from our case.

The correlation length also shows an interesting behavior. In the heating cycle between 50 and 150 K, the peak intensity reaches a maximum around 70 K, and the correlation length shows the largest values at a slightly higher temperature, These results mean that as long as the peak intensity increases, the correlation length also increases. In this temperature region, the domain dynamics get slower and the domains become larger. After the peak intensity reaches maximum, the correlation length is hardly affected, but the peak intensity starts to decrease. This means that the fluctuations for an individual atomic site are increasing, but the domain size remains stable and the domain walls are locked. This result shows that there is a clear connection among the improved order (maximal intensity), the correlation (maximal correlation length), and the largest *h*. To test if this relation is quantitatively the same for cooling and heating cycles, we show in panel (d) the correlation length as a function of peak position.

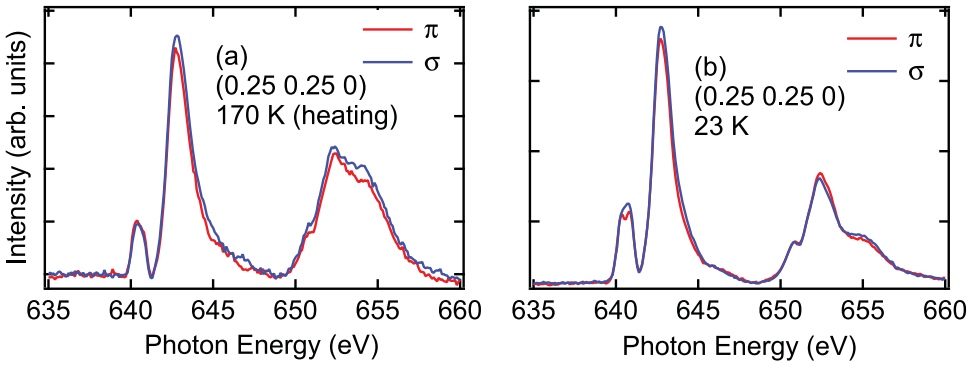

Figure 4. Intensity of the (hh0) (h = 0.25) peak as a function of photon energies at the Mn $2p \rightarrow 3d$ absorption edge at 170 K in the heating cycle (a) and 23 K (b).

Although the length is linearly dependent on the peak position for both the cooling and the heating cycles, the slope of the two is significantly different. A single slope seems to describe the data, except those view points above 180 K in the heating cycle, where the decay of the intensity is rather steep. The hysteresis is a clear representation of the first-order character of this phase transition, and this character is more pronounced, probably due to the interplay between the metallic LSMO and the insulating PCMO layers.

Figure 4 shows the spectral shape of the (hh0) reflection in the vicinity of the Mn $2p$ edges at 170 K in the heating cycle (a) and 23 K (b). In both of these cases, the value of h is 0.25. There is no polarization dependence at both temperatures. In addition, the spectral shape at the Mn $2p_{3/2}$ edge is identical at these two temperatures and similar to the pure orbital scattering of the analogue reflection in bulk $La_{1.5}Sr_{0.5}MnO_4$ [24, 25, 27] and the pure PCMO thin film [33]. The difference of the spectral shape at the Mn $2p_{1/2}$ edge comes from the q-independent fluorescence and diffuse scattering, which affects weak (hh0) peak intensity at 170 K. In other words, we find no indication of magnetic scattering in the superlattice, in contrast to the pure PCMO thin film [33]. There, RSXD study revealed two magnetic transitions: T_N = 150 K and T_2 = 75 K. The magnetic intensity of the (hh0) reflection in the film and the bulk can be directly related to a spin canting of the Mn spins along the c axis, which is clearly absent in the superlattice. Nevertheless, the maximum intensity in the heating cycle occurring around 70 K coincides with the magnetic transition of the pure PCMO thin film. In bulk (La,Pr,Ca)MnO_3 systems, this 70-K magnetic transition is much more pronounced [38] and is believed to be caused by a phase separation between FM and AF phases with glassy character at low temperatures. Such a phase transition would also be directly visible in the observed orbital reflection intensities. The difference between the PCMO thin film and the corresponding bulk material indicates that the epitaxial strain affects the magnetism in thin films [33]. The observation of the 70-K transition in the orbital signal in the superlattice is indirect evidence that the superlattice is AF with spins lying fully in the ab-plane, as observed by neutron diffraction on PCMO bulk samples [10].

We also obtained information on the metalicity from the Mn $2p_{3/2}$ HXPES spectra as shown in figure 5. Panels (a) and (b) show the temperature dependence, where a large hysteresis is observed between heating (a) and cooling (b) cycles. One can see that a lower-binding-energy feature is centered around 639.5 eV and is temperature-dependent. This structure was reported in $La_{1-x}Sr_xMnO_3$ [39], La_{1-x} Ba_xMnO_3 [40, 41], and $La_{1.2}Sr_{1.8}Mn_2O_7$ [42], and was considered

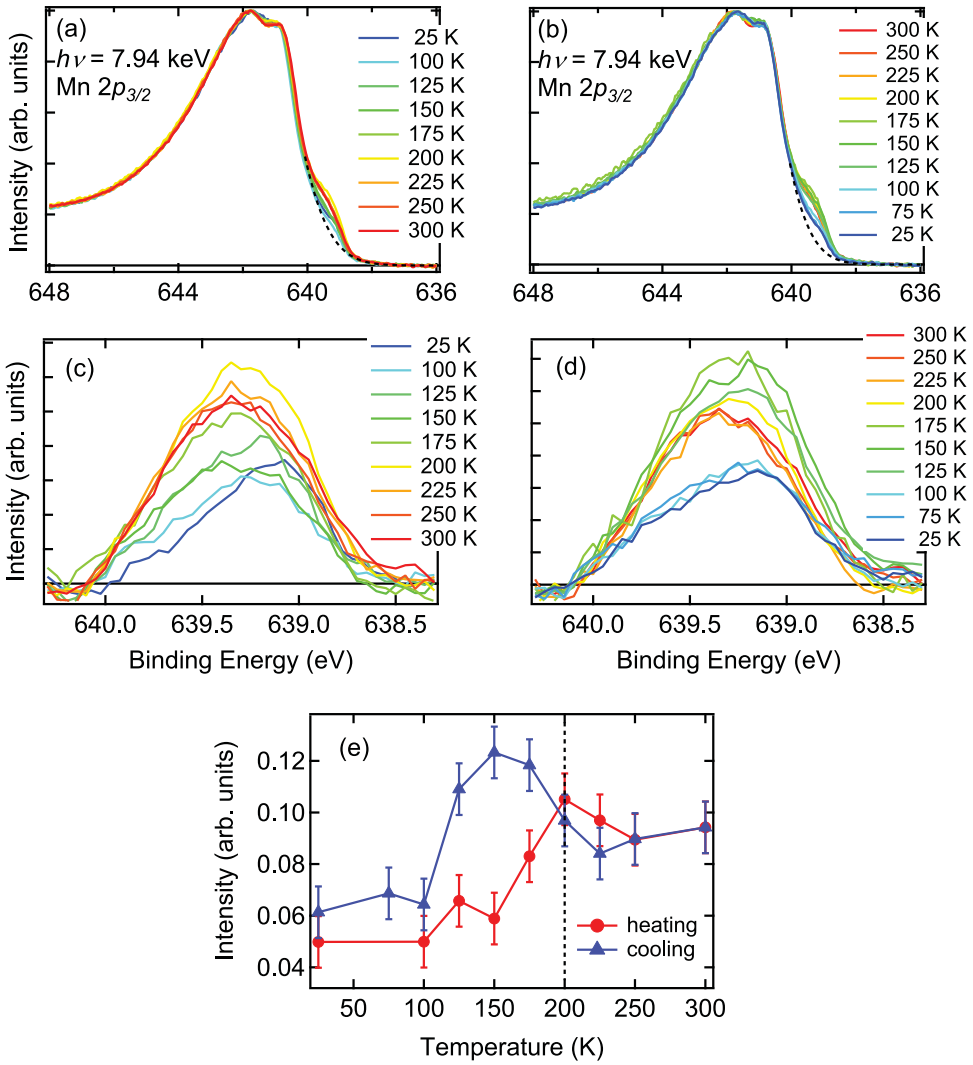

Figure 5. Temperature dependence of the Mn $2p_{3/2}$ HXPES spectra in the heating (a) and cooling (b) cycles. The dashed lines show the tail of the Mn $2p_{3/2}$ main structure approximated by Gaussian functions. Screened peaks after subtraction of the main structures are shown in the heating (c) and cooling (d) cycles. Panel (e) shows the intensity of the screened peak as a function of temperature.

a well-screened peak due to the existence of metallic carriers. The temperature dependence of this structure is shown in panels (c) and (d) after Gaussian background subtraction at panels (a) and (b), respectively. Panel (e) shows the screened-peak intensity obtained from the area in panels (c) and (d). The intensity shows a large hysteresis, especially between 100 and 200 K, where RSXD also shows a large hysteresis. The screened-peak intensity is lowest at 25 K. At this temperature, PCMO shows CO/OO states with a long correlation length, and the sample is most insulating. In the heating cycle, the intensity increases when the CO/OO states in the PCMO layers start to become weak, and reaches the highest intensity at 200 K, where the CO/OO states completely disappear. In the cooling cycle, the intensity shows higher values than in the heating cycle between 100 and 200 K, corresponding to the slow emergence of the CO/OO

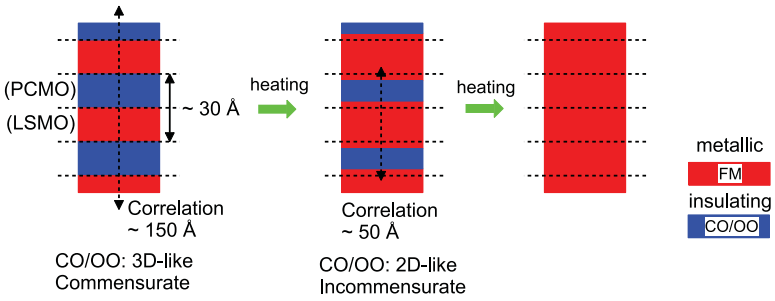

Figure 6. Proposed real-space sketches for the multilayer at different temperatures (or temperature cycle history). Ferromagnetic interfaces lead to charge transfer and to a reduction of the 3*d* coupling of the orbital order, represented by incommensurability and dynamics reducing the correlation length.

states in the PCMO layers. At 25 K, the intensity comes back to the original value within experimental error bars.

Combining our data with the results from [18] leads now to the following picture. The proposed phase separation between the FM LSMO layers and the orbital-ordered AF insulating PCMO layers is supported by the observation of the ferromagnetic moment [18], the orbital reflection by RSXD, and the metallic carriers by HXPES. At 25 K, a correlation length is about ~300 Å from figure 3(b), giving the effective correlation length perpendicular to the film surface of ~300 cos (60°) Å = 150 Å, where cos (60°) comes from the geometry in figure 1. The correlation length of ~150 Å indicates that the correlation between the CO/OO states perfectly bridges the FM layers built in between, making the CO/OO states 3D. (One unit of [PCMO (5 layers)/LSMO (5 layers)] is ~30 Å.) This is visualized in the left panel of figure 6. This orbital coupling bridging over the FM LSMO layers becomes weak when the temperature increases, because the interface CO/OO states disappear first, leading to an effective increase of the separation of the CO/OO layers as shown in the middle panel of figure 6. Near 200 K, the effective correlation length becomes as short as ~100 cos (60°) Å = 50 Å as seen in figure 3(b). This can cover fewer than two units of [PCMO (5 layers)/LSMO (5 layers)], making the CO/OO states 2D-like. The proximity effect (charge transfer between the layers) leads to a slight change of the overall doping in the CO/OO layers, which can explain the change in the ordering wave vectors. This was supported by the fact that, in some of CO/OO manganite systems, there is a direct relation between the doping level and the orbital- and charge-ordering periodicity due to Coulomb repulsion. For example, in 2/3 doped $Tb_{0.66}Ca_{0.33}$ $BaMn_2O_6$ [29], due to the A-site order in layers, a similar 2D character exists in the bulk (though with much shorter distances). Also, in these systems, competition between FM/AF ordering exists, and for a wide range of doping, a change of ordering vector and correlation length has been interpreted in terms of a decoupling between the orbital-ordered layers.

4. Summary

In summary, we performed RSXD and HXPES measurements on the superlattice of charge-ordered insulating PCMO and ferromagnetic metallic LSMO to study the charge-orbital ordering in the PCMO layers and the metallic carriers in the LSMO layers. We found that the behaviours of the superlattice are clearly different from those of the pure PCMO and LSMO

thin films. A direct correlation between the degree of electronic order (the expectation value of orbital occupation) and the correlation between the orientation of the orbitals (correlation length) and the period of the ordering (ordering wave vector) is observed. It shows that orbital order in the insulating AF PCMO coherently bridges the FM LSMO layers. With heating, we observed a reduction of orbital order at the interface by RSXD, and the increase of the metallic carriers by HXPES. This leads to a weakening of the interaction through the FM layers and an effective doping due to charge transfer. That results in a change in wave vector and a reduction of the correlation length due to the increase in dynamics common in 2D systems.

Acknowledgments

The authors thank the experimental support of the X11MA beam line staff. Financial support from the Swiss National Science Foundation and its NCCR MaNEP is gratefully acknowledged. This research is also granted by the Japan Society for the Promotion of Science (JSPS) through the 'Funding Program for World-Leading Innovative R&D on Science and Technology (FIRST Program),' initiated by the Council for Science and Technology Policy (CSTP). The synchrotron radiation experiments at SPring-8 were performed under the approval of the Japan Synchrotron Radiation Research Institute (2011A1624).

References

[1] Imada M, Fujimori A and Tokura Y 1998 *Rev. Mod. Phys.* **70** 1039
[2] Ramirez A P 1997 *J. Phys.: Condens. Matter* **9** 8171
[3] Tokura Y and Nagaosa N 2000 *Science* **288** 462
[4] Rao C N R, Arulraj A, Cheetham A K and Raveau B 2000 *J. Phys.: Condens. Matter* **12** R83
[5] Prellier W, Lecoeur P and Mercey B 2001 *J. Phys.: Condens Matter* **13** R915
[6] Dagotto E, Hotta T and Moreo A 2001 *Phys. Rep.* **344** 1
[7] Haghiri-Gosnet A M and Renard J P 2003 *J. Phys. D: Appl. Phys.* **36** R127
[8] Tokura Y 2006 *Rep. Prog. Phys.* **69** 797
[9] Urushibara A, Moritomo Y, Arima T, Asamitsu A, Kido G and Tokura Y 1995 *Phys. Rev.* B **51** 14103
[10] Jirak Z, Krupicka S, Simsa Z, Dlouha M and Vratislav S 1985 *J. Magn. Magn. Mater.* **53** 153
[11] Milward G C, Calderon M J and Littlewood P B 2005 *Nature* **433** 607
[12] Shimomura S, Tonegawa T, Tajima K, Wakabayashi N, Ikeda N, Shobu T, Noda Y, Tomioka Y and Tokura Y 2000 *Phys. Rev.* B **62** 3875
[13] Izumi M, Konishi Y, Nishihara T, Hayashi S, Shinohara M, Kawasaki M and Tokura Y 1998 *Appl. Phys. Lett.* **73** 2497
[14] Horiba K, Chikamatsu A, Kumigashira H, Oshima M, Nakagawa N, Lippmaa M, Ono K, Kawasaki M and Koinuma H 2005 *Phys. Rev.* B **71** 155420
[15] Nakamura M, Ogimoto Y, Tamaru H, Izumi M and Miyano K 2005 *Appl. Phys. Lett.* **86** 182504
[16] Wakabayashi Y, Bizen D, Nakao H, Murakami Y, Nakamura M, Ogimoto Y, Miyano K and Sawa H 2006 *Phys. Rev. Lett.* **96** 017202
[17] Okuyama D, Nakamura M, Wakabayashi Y, Itoh H, Kumai R, Yamada H, Taguchi Y, Arima T, Kawasaki M and Tokura Y 2009 *Appl. Phys. Lett.* **95** 152502
[18] Nakamura M, Okuyama D, Lee J S, Arima T, Wakabayashi Y, Kumai R, Kawasaki M and Tokura Y 2010 *Adv. Mater.* **22** 500
[19] Murakami Y, Kawada H, Kawata H, Tanaka M, Arima T, Moritomo Y and Tokura Y 1998 *Phys. Rev. Lett.* **80** 1932

[20] Ishihara S and Maekawa S 1998 *Phys. Rev. Lett.* **80** 3799
[21] Elfimov I S, Anisimov V I and Sawatzky G A 1999 *Phys. Rev. Lett.* **82** 4264
[22] Benfatto M, Joly Y and Natoli C R 1999 *Phys. Rev. Lett.* **83** 636
[23] Wilkins S B, Hatton P D, Roper M D, Prabhakaran D and Boothroyd A T 2003 *Phys. Rev. Lett.* **90** 187201
[24] Wilkins S B, Spencer P D, Hatton P D, Collins S P, Roper M D, Prabhakaran D and Boothroyd A T 2003 *Phys. Rev. Lett.* **91** 167205
[25] Dhesi S S *et al* 2004 *Phys. Rev. Lett.* **92** 056403
[26] Thomas K J *et al* 2004 *Phys. Rev. Lett.* **92** 237204
[27] Wilkins S B, Beale T A W, Hatton P D, Purton J A, Bencok P, Prabhakaran D and Boothroyd A T 2005 *New J. Phys.* **7** 80
[28] Staub U, Garcia-Fernandez M, Bodenthin Y, Scagnoli V, Souza R A D, Garganourakis M, Pomjakushina E and Conder K 2009 *Phys. Rev.* B **79** 224419
[29] Garcia-Fernandez M, Staub U, Bodenthin Y, Scagnoli V, Pomjakushin V, Lovesey S W, Mirone A, Herrero-Martin J, Piamonteze C and Pomjakushina E 2009 *Phys. Rev. Lett.* **103** 097205
[30] Zhou S Y *et al* 2011 *Phys. Rev. Lett.* **106** 186404
[31] Wadati H *et al* 2012 *Phys. Rev. Lett.* **108** 047203
[32] Garganourakis M, Scagnoli V, Huang S W, Staub U, Wadati H, Nakamura M, Guzenko V A, Kawasaki M and Tokura Y 2012 *Phys. Rev. Lett.* **109** 157203
[33] Wadati H, Geck J, Schierle E, Sutarto R, He F, Hawthorn D G, Nakamura M, Kawasaki M, Tokura Y and Sawatzky G A 2014 *New J. Phys.* **16** 033006
[34] Scagnoli V, Staub U, Mulders A M, Janousch M, Meijer G I, Hammerl G, Tonnerre J M and Stojic N 2006 *Phys. Rev.* B **73** 100409(R)
[35] Staub U, Scagnoli V, Bodenthin Y, Garcia-Fernandez M, Wetter R, Mulders A M, Grimmer H and Horisberger M 2008 *J. Synchroton Radiat.* **15** 469
[36] Flechsig U, AlsNielsen J, Jaggi A, Krempasky J, Oberta P, Spielmann S and van der Veen J F 2010 *AIP Conf. Proc.* **1234** p 653
[37] Niebieskikwiat D, Hueso L E, Borchers J A, Mathur N D and Salamon M B 2007 *Phys. Rev. Lett.* **99** 247207
[38] Wu W, Israel C, Hur N, Park S, Cheong S-W and de Lozanne A 2005 *Nat. Mater.* **5** 881
[39] Horiba K *et al* 2004 *Phys. Rev. Lett.* **93** 236401
[40] Tanaka H *et al* 2006 *Phys. Rev.* B **73** 094403
[41] Ueda S, Tanaka H, Ikenaga E, Kim J J, Ishikawa T, Kawai T and Kobayashi K 2009 *Phys. Rev.* B **80** 092402
[42] Offi F *et al* 2007 *Phys. Rev.* B **75** 014422